Investigation of the Adsorption of Methanol on Alkali Metal Cation Exchanged Zeolite X by Inelastic Neutron Scattering

Renate Schenkel,[†] Andreas Jentys,*[,†] Stewart F. Parker,[‡] and Johannes A. Lercher[†]

Institut für Technische Chemie, Technische Universität München, 85747 Garching, Germany and ISIS Facility, Rutherford Appleton Laboratory, Chilton, Didcot, Oxon OX11 0QX, United Kingdom

Received: January 14, 2004; In Final Form: March 29, 2004

The adsorption of methanol on alkali metal cation exchanged zeolite X was studied by inelastic neutron scattering (INS) and Fourier transform infrared (FTIR) spectroscopy in the range 30−2000 and 1300−3800 cm^{-1}, respectively. Infrared vibrational spectra from solid methanol and methanol adsorbed on the zeolites were compared to INS spectra calculated from ab initio simulations for one, two, and three methanol aggregates to describe the interactions between the sorbate molecules and the zeolite. Solid methanol was found to crystallize in the low temperature α-phase by instant cooling to temperatures below 20 K. The primary interaction of methanol and the zeolite occurred between the oxygen atom of the alcohol and the cations located at the ion exchange positions of the zeolite. The increasing shift of the ν(OH) stretching vibration with increasing framework polarity of the zeolite indicates additional interaction between the OH group of methanol and the lattice oxygen atoms as well as intermolecular hydrogen bonding between adjacent adsorbed methanol molecules.

Introduction

Catalysts with pronounced basic properties are able to catalyze a large number of reactions including olefin isomerization, aldehyde and ketone condensation, side chain alkylaromatic alkylation, dehydrogenation, and amination. Crystalline microporous materials such as zeolites are used as catalysts for acid−base catalyzed reactions[1] as they can be prepared with well-defined and isolated acid/base sites[2] in combination with a wide range of pore dimensions[3] matching the size of the organic reactants. This allows the chemical reactions to take place in a specifically chosen and well-defined environment (i.e., in the cages or channels of the molecular sieves, which act as nano scale reactors). To improve reaction yields and selectivities, knowledge of the chemical and structural properties of the active sites and their relation to the sorbent−sorbate structure is essential for a rational catalyst design.

For the alkylation of toluene with methanol, it was found that zeolites with predominately basic properties catalyze side chain alkylation (i.e., the formation of styrene and ethylbenzene), while on zeolites with acid sites, a high selectivity to the formation of xylenes (alkylation of the aromatic ring) was observed.[4] A systematic study of the (nonreactive) interaction of methanol with alkali metal cation exchanged molecular sieves using in situ IR spectroscopy performed by Rep et al.[5] showed that with increasing framework polarity (i.e., decreasing Si/Al ratio and/or increasing atomic size of the exchanged cations), the interaction between methanol and lattice oxygen atoms of the zeolite via the hydrogen atoms of the hydroxyl group and the methyl groups increased. This was attributed to the increase in the negative charge of the framework oxygen atoms located at the inner surface of the zeolite. However, the direct interaction between the lone pair electron donor function of methanol via the oxygen atom of the hydroxyl group and the electron pair acceptor function of the zeolite (i.e., the alkali metal cations) has been identified as the most important energetic contribution to sorption. The size of the metal cations in the molecular sieve controls the preference for the sorption of methanol versus toluene with the smaller cations having a greater preference for methanol than the larger. While the principle features of these interactions are known, our knowledge of the complex adsorption structures of methanol in these polar materials is still rudimentary.

In this work, we wish to further explore the complex interaction of methanol with alkali metal cation (Na^+, K^+, Rb^+, Cs^+) exchanged zeolite X. Zeolite X belongs to the faujasite structural group (FAU) consisting of a three-dimensional pore system with large supercages and 12 MR-pore openings, which are easily accessible for sorbates. The role of the zeolite basicity on the sorption of methanol was studied by inelastic neutron scattering (INS) and infrared (IR) spectroscopy, and potential sorption structures are discussed. The reason for this choice of the spectroscopy is based on the differences between IR and INS spectroscopy. Infrared intensities are determined by the interaction of electromagnetic radiation with the electrons present in the system, while for inelastic neutron scattering the intensity depends on the momentum transfer, the amplitude of vibration, and the incoherent scattering cross-section. Because the cross-section of hydrogen is 10−100 times larger than that of all other elements and being the lightest element, its amplitude of vibration in large motions involving hydrogen dominate the INS spectrum.

Experimental Procedures

Materials. Commercial NaX zeolite (Si/Al = 1.3; Köstrolith, Südchemie) was exchanged with 0.1 molar alkali metal nitrate solutions (Na^+, K^+, Rb^+, and Cs^+). The suspension was stirred at 535 K for 20 h (solid/liquid ratio = 20 g L^{-1}), cooled to room temperature, washed, dried, and subsequently calcined at 723 K under flowing synthetic air for 1 h. The complete

[†] Technische Universität München.
[‡] Rutherford Appleton Laboratory.

10.1021/jp049819f CCC: $27.50
Published on Web 05/13/2004

TABLE 1: Si/Al Ratio, Degree of Ion Exchange, Calculated Unit Cell Composition, Micropore Volume, Calculated Average Charge on the Oxygen of the Lattice ($-\delta_0$), and the Electrostatic Potential of Sodium Cation (e/r) of Alkali Metal Cation Exchanged X Zeolites Determined from AAS Analysis and N_2-Sorption Studies

sample	Si/Al	M^+/Al [mol %]	Na^+/Al [mol %]	unit cell composition	micropore volume [m^3/g]	S_{int} [a]	$-\delta_0$ [b]	e/r [Å^{-1}]
NaX	1.2	100	100	$Na_{88}Al_{88}Si_{104}O_{384}$	0.17	2.314	0.337	1.05
KX	1.3	95.3	2.3	$K_{82}Na_2Al_{84}Si_{108}O_{384}$	0.15	2.298	0.341	0.75
RbX	1.2	67.5	32.5	$Rb_{60}Na_{29}Al_{88}Si_{104}O_{384}$	0.11	2.232	0.358	0.67
CsX	1.3	55.4	44.6	$Cs_{47}Na_{38}Al_{85}Si_{107}O_{384}$	0.10	2.239	0.356	0.59

[a] $S_{int} = (S_P{}^p S_Q{}^q S_R{}^r S_T{}^t)^{1/(p+q+r+t)}$: for a compound $P_pQ_qR_rT_t$ calculated intermediate Sanderson electronegativity.[10,11] [b] Calculated average charge $-\delta_o$ on the oxygen of the lattice, using $(S_{int} - S_o)2.08S_o^{1/2}$.

exchange procedure was repeated three times. Cs^+ ion exchange was performed by IKO minerals. The composition of the materials and the pore volume determined by AAS and N_2-sorption, respectively, are summarized in Table 1.

INS Experiments and Sample Preparation. Inelastic neutron scattering measurements were performed on the spectrometer TOSCA at the spallation neutron source ISIS (Rutherford Appleton Laboratory, U.K.). TOSCA uses an indirect time-of-flight geometry that allows inelastic neutron scattering spectra to be recorded in the energy transfer range of 30−4000 cm^{-1} with a resolution of $(\Delta E/E) \sim 1.5\%$.[6]

The zeolite samples were activated under flowing synthetic air at 723 K for 4 h. Sorption of methanol with a loading of three molecules per supercage (corresponding to a coverage 0.27% of the countercations) was performed at 308 K in helium as carrier gas. Subsequently, 20 g of the zeolite powder was transferred into the sample containers made from aluminum (size 45 × 50 × 20 mm) under inert atmosphere. The cells were sealed and heated to 353 K for 24 h to equilibrate the sorbate. Liquid samples were investigated in flat thin-walled aluminum cells. For recording the spectra, the sample containers were placed in a helium cryostat and cooled to ca. 20 K. The spectra were recorded at temperatures below 20 K in the energy range of 30−4000 cm^{-1}, and measurement times were typically ~10 h. The spectrum of an empty container and of the activated zeolite was subtracted from the spectra of the samples. In general, the activated zeolite samples are weak neutron scatterers; therefore, all intensity observed after the sorption results from the H atoms in the methanol molecules.

IR Experiments. The sorption experiments were followed by in situ IR spectroscopy (Bruker IFS-88, resolution 4 cm^{-1}) at 308 K and methanol partial pressures of 10^{-3} mbar. The samples were pressed into self-supporting wafers (ca. 5 mg) and activated in a vacuum ($p < 10^{-6}$ mbar) with a heating rate of 10 K min^{-1} up to 723 K (holding for 30 min). The spectra were recorded in the transmission absorption mode and monitored time-resolved during equilibration of the zeolite sample with the sorbate. All spectra were baseline corrected between 3800 and 1100 cm^{-1} and normalized to the integral peak area of the overtones of the framework vibrations in the range of 2100−1735 cm^{-1}. The spectra presented in this paper are difference spectra (i.e., the spectrum of the activated zeolite is subtracted from the spectrum of the zeolite after adsorption of methanol). In this mode of presentation, IR bands pointing upward increased in intensity and band pointing downward decreased in intensity upon the interaction of the zeolite with methanol.

Computational Methods. The structure of single methanol molecules and of clusters consisting of two and three methanol molecules were optimized with respect to the total energy using density functional theory (DFT) as implemented in *Gaussian 98*.[7] The 6-31G** basis set and nonlocal corrections on the B3LYP level were applied. After having achieved the optimized geometry for the different clusters investigated, the vibrational modes were calculated. The displacement vectors determined for each vibrational mode were used to simulate the INS (including lattice modes and overtone vibrations) using the program a-CLIMAX.[8]

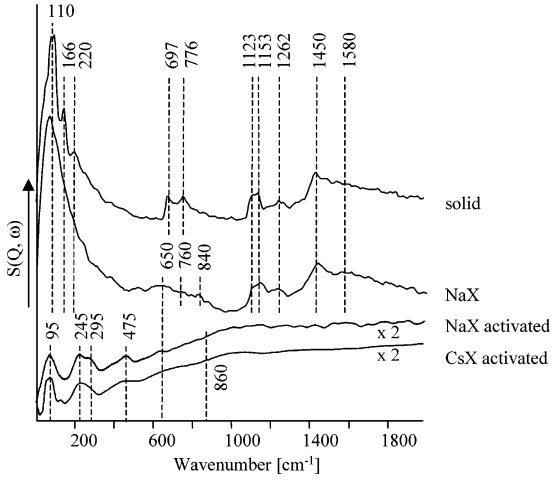

Figure 1. Inelastic neutron scattering spectra of dehydrated NaX and CsX, methanol adsorbed on NaX (loading three molecules per supercage, on average), and solid methanol at $T < 20$ K.

Results

Dehydrated Alkali Metal Cation Exchanged X Zeolites. The chemical composition and structural properties of the alkali cation exchanged zeolites are summarized in Table 1. For INS, the spectra had to be collected at very low temperatures (<20 K) to reduce the dynamic disorder, which has been measured for molecules chemisorbed in zeolites.[9] The average partial negative charge of the framework oxygen atoms in the differently ion exchanged zeolites were estimated using the Sanderson intermediate electronegativity principle.[10,11] The results clearly show that the negative oxygen partial charge $-\delta_0$ increases with increasing size of the monovalent cations; thus, Rb^+- and Cs^+-exchanged zeolite X were the most basic samples in the series of material studied.

The INS spectra of solid methanol, of the dehydrated NaX sample, and of methanol adsorbed on NaX are shown in Figure 1. In the region of the $\nu(CH_3)$ stretching vibrations (around 3000 cm^{-1}) and of the ν(OH) stretching vibrations (around 3500 cm^{-1}), only broad and unresolved bands of low intensity were observed due to the high momentum transfer; therefore, this region was not further analyzed. The INS spectra of the dehydrated NaX zeolite is very similar to the spectrum of a completely cation exchanged NaY reported by Jobic et al.[12] The band at 95 cm^{-1} is located in the region of external unit cell modes (e.g. translational and rotational lattice modes and translation modes of cations to the framework).[13] The broadened band at 200−300 cm^{-1} is attributed to pore opening vibrations.[14]

TABLE 2: Experimental Vibrational Frequencies and Their Assignments of the INS Bands of Methanol in the Solid and Adsorbed (3 methanol molecules per faujasite supercage, on average) State (T < 20 K), Together with the Vibrational Frequencies of Methanol Clusters Calculated by DFT

DFT[a]				IR[c]	INS[a]
monomer	linear dimer	cyclic trimer	assignment[b,d]	crystal	solid phase
	1530 (d)	1530, 1529, 1528, 1505	$\delta_s(CH_3) + \delta(OH)_{ip}$	1458 sh, 1445 sh m, 1426 sh	several bands with maxima at 1476 sh and 1450
1527, 1509	1523, 1513, 1508 (d)	1511, 1510, 1509	$\delta_{as}(CH_3)$		
1499	1500 (d), 1492	1495, 1494, 1490	$\delta_s(CH_3)$		
1386	1445 (d), 1373	1464, 1445	$\delta(OH)_{ip}$	1470 (1492)[e] m	
1179	1182	1184, 1183	$\rho(CH_3)_{rock}$	1256 w, 1162 vw, 1142 w	1255, 1154, 1130
1095, 1062	1127 (d), 1082	1176, 1142, 1128	$\rho(CH_3)_{rock} + \delta(OH)_{ip}$		
	1089 (d), 1056 w	1091 w, 1074, 1072	ν(CO)	1046 w, 1029 vw	1021 w
	729 (d)	964, 785, 732	$\delta(OH)_{op}$	790 (824)[e] s, 685 (698)[e]	776, 697
340	332		$\delta(OH)_{op}$		
	217	240, 232, 218	ν(OH···O)		220
	137, 109	173, 124, 121, 116, 109	$\tau(CH_3)$ + translation		168, 110
	87, 72, 44	97, 59, 52, 44	intermolecular	166, 110 s	
1045, 696, 1400	1458, 776, 663	1301, 1234, 1016, 904, 832, 296, 348	overtones and combination modes	1545 sh vw, 1345m, 520 w, 372[e] m	1288, 340 w, 284 w

[a] This paper. [b] All frequencies are in cm^{-1}; vs = very strong, s = strong, m = medium, w = weak, vw = very weak, sh = shoulder, and br = broad. [c] See ref 18. [d] aCLIMAX fit to methanol DFT data. [e] Frequencies extrapolated to 0 K.

The feature in the region of 300−500 cm^{-1} is assigned to the T−O−T bending vibration (T denotes tetrahedrally coordinated Si or Al atoms), while the weak bands between 600 and 800 cm^{-1} and above 950 cm^{-1} are assigned to symmetric and asymmetric ν(T−O) stretching vibrations of T−O−T units, respectively.[13,15] The very weak shoulder around 860 cm^{-1} is assigned to the hydroxyl bending vibrations of terminal silanol groups.[16] In general, the intensities of the INS bands observed for the dehydrated samples were small, and moreover, significant differences were not observed for the different alkali metal cation exchanged samples investigated.

The infrared spectrum of NaX in the activated form showed the typical bands of OH stretching vibrations for terminal and internal Si−OH groups at 3748 and 3720 cm^{-1}, respectively, as well as OH groups of extraframework aluminum species 3669 cm^{-1}, while OH stretching vibrations of Si(OH)Al groups (i.e., Brønsted acidic bridging hydroxyl groups) were not observed. In addition, bands of structural overtone vibrations were present between 2100 and 1735 cm^{-1}, which were used to normalize all IR spectra shown in this paper.

Solid Methanol. The vibrational modes calculated for methanol and obtained experimentally for solid methanol are compared to data from the literature in Table 2. The INS spectrum of solid methanol (see Figure 1 and Table 2) with bands arising at 1450, 1262, 1153, 1123, 776, 697, 220, 166, 110, and 76 (shoulder) cm^{-1} is in good agreement with the spectrum reported by Jobic et al.[17] The symmetric and asymmetric δ(OH) and δ(CH) deformation modes are located in the region of 1380−1520 cm^{-1} with a maximum at 1450 cm^{-1}, which is due to the three unresolved $\delta(CH_3)$ bending modes. The very weak signal at 1021 cm^{-1} is assigned to the ν(CO) stretching mode[18] only marginally red shifted from the gas-phase value at 1033 cm^{-1}, while the broad band in the region of 1100−1160 cm^{-1} is assigned to $\rho(CH_3)$ rocking modes and their combinations with δ(OH) bending modes. Both signals at 697 and 776 cm^{-1} are due to $\delta(OH)_{op}$ modes attributed to hydrogen bonded hydroxyl groups of larger methanol clusters, similar to those found by infrared spectroscopy for crystalline methanol[18] in the low temperature α-phase.[19] The shift of the bands observed by INS as compared to those obtained by IR spectroscopy (790 and 685 cm^{-1})[18] is attributed to the higher temperature (93 K) used for the IR measurements, while both frequencies are lower as compared to the data reported by Jobic et al.[17] obtained at 5 K. In the lower energy region, a broad and very intense band with a maximum at 110 cm^{-1} and shoulders at 57, 76, 168, and 220 cm^{-1} was observed, which is assigned to strongly overlapping translational and librational modes and to hydrogen bond bending modes.

Adsorption of Methanol on Sodium Exchanged Zeolite X. The INS spectrum of methanol adsorbed on NaX is shown in Figure 1, and the assignment of the vibration modes is summarized in Table 3. The INS spectrum of methanol absorbed on NaX exhibited several broad bands in the methyl and hydroxyl in-plane deformation region (1350−1530 cm^{-1}) and in the methyl rocking region (1080−1180 cm^{-1}). The band at 1447 cm^{-1} was assigned to the (poorly resolved) $\delta(CH_3)$ bending vibrations, the bands at 1160 and 1115 cm^{-1} (shoulder) were assigned to $\rho(CH_3)$ rocking modes possibly combined with δ(OH) bending modes. The positions of the bands in both regions are similar to those observed for solid methanol. The significant broadening of those bands shows that there is no long-range order and may also indicate a perturbation of the methanol−methyl groups. The broad band centered at 1580 cm^{-1} is attributed to the combination band of the methyl vibration modes and low-frequency external modes of the methanol molecules. The $\delta(OH)_{op}$ deformation vibration modes of hydrogen-bonded hydroxyl groups were observed between 500 and 900 cm^{-1}. One broad band was obtained between 600 and 700 cm^{-1} centered at 650 cm^{-1}, and another weak band was located at ∼760 cm^{-1}. The lower value was at a similar position to that found for liquid methanol (655 cm^{-1}).[18] The very intense and unresolved band in the low energy region below 450 cm^{-1} resulted from translational and librational modes of methanol against the zeolite framework as well as from hydrogen bond bending and stretching modes.

Calculated Vibrational Frequencies of Methanol and Methanol Cluster. The INS spectra simulated for a single methanol molecule, a cluster of two molecules forming a linear dimer, and three molecules oriented as a cyclic trimer cluster are shown in Figure 2. The vibrational modes in an isolated methanol molecule are compared to those in hydrogen bonded dimeric and trimeric methanol clusters in Table 2. The orientation of the methanol molecules in the clusters has been chosen because theoretical calculations[20−22] and experimental results[23−25] have shown that the methanol dimers form linear clusters, while trimer to decamer structures form stable monocyclic clusters.

The spectrum of the single methanol molecule presented eight fundamental vibrations and several overtone vibrations in the

TABLE 3: Experimental Vibrational Frequencies and Their Assignments of the INS Bands of Methanol Adsorbed on Alkali Metal Cation Exchanged X Zeolites (Loading 3 Molecules per Supercage, on Average) at $T < 20$ K

assignment[a]	methanol on NaX	methanol on KX	methanol on RbX	methanol on CsX
$\delta(OH)_{ip}$ and $\delta(CH_3)_{ip}$	1580 br, 1450	1580 br, 1460	1900−1400 br m 1580 br, 1460	1580 br, 1460
$\rho(CH_3)_{rock}$	1160, 1115	1160, 1125	1100−1180 br m 1160, 1130	1160, 1130
$\nu(CO)$	1018 vw	1040 vw	1020 vw	1015 vw
$\delta(OH)_{op}$ H-bound	650, 760	765, 810	900−500 br m 765, 820	765, 820
$\tau(CH_3)$ and translation of methanol and methanol−cation cluster	263 sh, 122 sh, 95 vs	263 sh w, 125 sh w, 98 vs	<450 br vs 263 sh w, 125 sh w, 100 vs	263 sh w, 130 sh w, 100 vs
overtones and combinations	1010, 845		1220−1250 w	

[a] All frequencies are in cm^{-1}; vs = very strong, s = strong, m = medium, w = weak, vw = very weak, sh = shoulder, and br = broad.

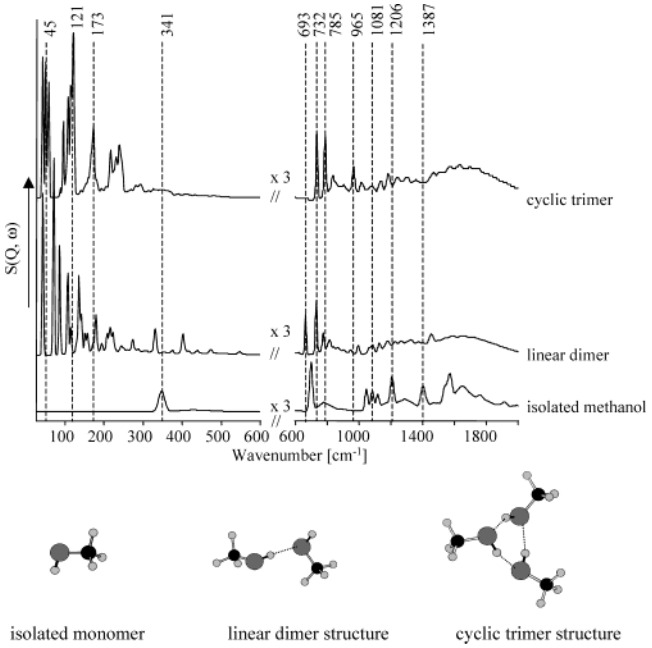

Figure 2. Calculated vibrational spectra and their equilibrium structures of (a) single methanol molecules, (b) linear dimmer, and (c) cyclic trimer clusters.

range between 30 and 2000 cm^{-1}. The bands at 348, 696, 1045, and 1400 cm^{-1} have been assigned to the $\delta(OH)_{op}$ deformation vibrations of the OH group and its first, second, and third overtone vibrations, respectively. The $\nu(CO)$ stretching vibration, the combination of the $\delta(OH)$ deformation with a $\rho(CH_3)$ rocking mode, and the pure $\rho(CH_3)$ rocking mode have been observed at 1081, 1116, and 1206 cm^{-1}, respectively. The in-plane $\delta(OH)_{ip}$ deformation vibration band was located at 1387 cm^{-1}, and several bands between 1450 and 1530 cm^{-1} result from $\delta(CH_3)$ bending deformation vibrations and from combination modes of $\delta(OH)_{op} + \delta(CH)$.

The simulated spectra of the hydrogen bonded linear dimer and the cyclic trimer cluster exhibited 15 and 35 fundamental modes, respectively, and an increased number of overtone and combination vibrations leading to strongly overlapped features. Both spectra have a large number of bands in the low energy region. In this region, the out-of-plane and in-plane bending modes of the hydrogen bonded molecules and the translations and librations of the entire methanol molecules are typically found. Those vibrations were mainly combined with translational modes of the molecules. The methanol−methyl torsion vibrations have been assigned to the bands at 108 and 137 cm^{-1} for the linear, hydrogen bonded methanol dimer and to several bands between 109 and 124 cm^{-1} for the hydrogen bonded cyclic trimer. The band at 173 cm^{-1} arose from a simultaneous torsion vibration of all three methanol−methyl groups.

For a cluster of two methanol molecules, the deformation vibration bands of the unperturbed as well as the hydrogen bonded hydroxyl groups $\delta(OH)_{op}$ were observed at 332 and 729 cm^{-1}, respectively. The two corresponding but very weak $\delta(OH)_{ip}$ deformation bands were seen at 1373 and 1445−1450 cm^{-1}. In the calculated spectrum of a cyclic trimer cluster, all hydroxyl groups were hydrogen bonded; therefore, no $\delta(OH)_{op}$ deformation band of a freely vibrating methanol hydroxyl group was found. The three bands, observed at 732, 785, and 963 cm^{-1}, have been assigned to hydroxyl deformation vibrations of hydrogen bonded hydroxyl groups. The first has been assigned to the vibration of a single hydroxyl group, while the latter two were due to two and three hydroxyl groups, respectively, vibrating simultaneously. An increasing number of overtone vibration bands and weak band intensities in the region above 1000 cm^{-1} led to strongly overlapped and not well-resolved bands. Besides the most prominent peaks, which have been ascribed mainly to the fundamental vibrations, several medium and small bands corresponding mostly to overtone and combination bands with fundamental vibrations were observed.

Adsorption of Methanol on Alkali Metal Cation Exchanged Zeolite X. The vibrational modes observed after methanol adsorption on the various alkali metal cation exchanged zeolites are shown in Figure 3 and summarized in Table 3. All materials exhibited a broad band between 1400 and 1500 cm^{-1} of strongly overlapping $\delta(OH)_{ip}$ and $\delta(CH)$ vibrations with a maximum at about 1460 cm^{-1}. The feature observed in the region of 1100−1180 cm^{-1} is associated with methyl rocking modes. All alkali cation exchanged materials have shown two bands at around 1115−1130 and 1160 cm^{-1}. The very weak band around 1018−40 cm^{-1} is assigned to the $\nu(CO)$ stretching mode only marginally red shifted from the gas-phase value at 1033 cm^{-1}.[15]

The most significant changes in the INS spectra of the alkali metal exchanged zeolites have been observed in the region of the out-of-plane deformation bending modes of the hydrogen-bonded hydroxyl groups. For NaX, a very broad band between 600 and 900 cm^{-1} was seen, and for samples with decreasing Lewis acidity (i.e., for K^+, Rb^+, and Cs^+ exchanged zeolite X), the width of these bands has decreased and shifted to 810 and 765 cm^{-1} for KX, 820 and 765 cm^{-1} for RbX, and 820 and 765 cm^{-1} for CsX. For samples with increasing cation size,

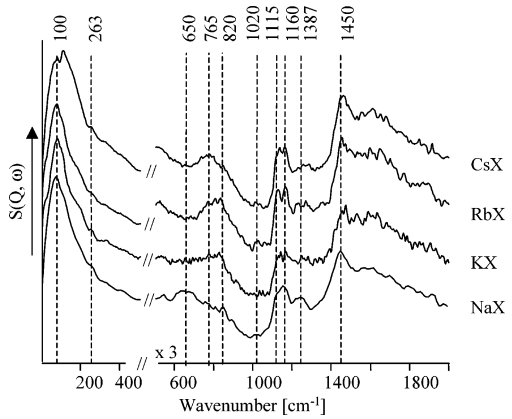

Figure 3. Inelastic neutron scattering spectra of methanol adsorbed on alkali metal cation exchanged X zeolites (loading three molecules per supercage, on average) at $T < 20$ K.

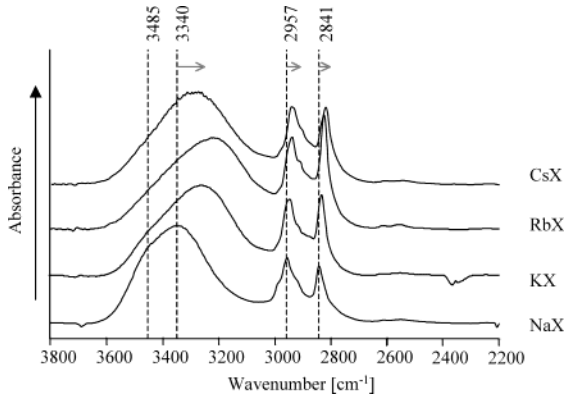

Figure 4. FTIR difference spectra of methanol adsorbed on alkali exchanged zeolite X ($T = 308$ K, $p(CH_3OH) = 1 \times 10^{-3}$ mbar).

the tail of the band below 450 cm^{-1} at higher frequencies (assigned to methyl torsion and the hydrogen bond bending and stretching modes, as well as to the translational and librational modes of the methanol−cation cluster to the zeolite and methanol to the cation) was more pronounced.

The infrared spectra after adsorption of methanol at a partial pressure of 10^{-3} mbar are shown in Figure 4. The frequencies of the OH stretching vibrations (summarized in Table 4) are broadened and strongly shifted to lower wavenumbers. The values vary for methanol adsorbed on the different alkali cation exchanged zeolite samples. The broad OH stretching vibration modes showed the highest frequency for methanol sorbed on NaX (3341 cm^{-1}) and decreased to lower wavenumbers for RbX (3219 cm^{-1}). For methanol adsorbed on CsX (3238 cm^{-1}), this band is observed at a somewhat higher value than for RbX. Similar to the OH stretching vibration, the antisymmetric and symmetric CH stretching vibration bands were found to be the highest in frequency for methanol sorbed on NaX (2957 and 2839 cm^{-1}, respectively) and decreased to the frequency of methanol sorbed on RbX and CsX (2934 and 2820−2823 cm^{-1}), respectively. The infrared data are in perfect agreement to the results reported by Rep et al.[5]

Discussion

Dehydrated Alkali Metal Cation Exchanged X Zeolites. The absence of bands around 420 and 1060 cm^{-1} as found for HNaY[12] (for HY predicted at 420 and 1110 cm^{-1} by quantum chemical calculations[26]) and in addition, the low intensities of the band above 480 cm^{-1} [12,27] clearly demonstrates the absence of Brønsted acid hydroxyl groups in all samples indicating complete cation exchange. The complete ion exchange is also confirmed by the chemical composition as well as by the absence of bands at 3640 and 3540 cm^{-1} assigned to OH stretching vibrations of Brønsted acid hydroxyl groups. The very low intensity of the shoulder around 860 cm^{-1}, which indicates terminal silanol groups,[16] demonstrates a low number of defects or extraframework phases.

Because of the similarity of the spectra observed for the different alkali metal cation exchanged samples after activation and the generally broad bands observed, a correlation between the exchange with cations and the structural changes of the framework could not be drawn. This may point to a minor influence of the countercation on the vibrational properties of the faujasite structure. Note that from infrared and Raman spectroscopy, shifts in the frequency of cation translational modes and framework bending modes were attributed to different countercation sizes and to slight structural changes of the framework upon exchange of the countercations.[28,29] From the INS spectrum of natrolite, a band at 40 cm^{-1} was assigned to sodium motion since it was present in both deuterated and hydrogenated spectra.[30] Because of the small scattering cross-section of the alkali metal cations, the translational modes of those cations are expected to be very weak in INS spectra and probably contribute to the band at 95 cm^{-1}. Note that the scattering of the sodium cations was found to be negligible for NaY materials.[31]

Solid Methanol. In analogy to the torsion vibration frequencies obtained in the simulation for the methanol clusters at around 109 and 173 cm^{-1}, the distinct maxima at 110 and 168 cm^{-1} in solid methanol are assigned to freely vibrating and hydrogen bonded methanol−methyl motions, respectively. From far-infrared and Raman studies at 88 K, Durig et al.[32] assigned the bands at 196, 160, 109, and 57 cm^{-1} to two in-plane and two out-of-plane hydrogen bond bending modes of solid methanol assuming C_2 symmetry for the methanol chain. The assignment from Durig et al.[32] is consistent with that of the methyl motion, as the methyl group, being the center of mass, must also move in the hydrogen bond bending motion. Aldred et al.[33] obtained a band at 160 cm^{-1} in the INS spectrum of methanol and assigned it to the methyl motion on the basis of the disappearance of the band after deuteration of the methyl group. In addition, the band at 270 cm^{-1} was assigned to a translational hydrogen bond stretching mode.[34]

TABLE 4: Vibrational IR Frequencies of Methanol Adsorbed on Alkali Metal Cation-exchanged X Zeolites ($T = 308$ K, $p(CH_3OH) = 1 \cdot 10^{-3}$ mbar)

assignment	gas phase[a]	liquid[b]	NaX	KX	RbX	CsX
ν(OH)	3682 s	3337 s, br	3460 sh, 3341 s, br	3453, 3255 s, br	3356 sh, 3219 s, br	3468 sh, 3238 s, br
$\nu(CH_3)$ as	2999, 2970	2934	2980 sh, 2957 br	2949, 2939	2947, 2934	2946, 2934
$\nu(CH_3)$ s	2844	2822	2839 br	2826	2820	2835 sh, 2823
$\delta_{as}(CH_3)$	1477, 1465, 1454	1475, 1453	1476, 1451	1479, 1450	1480, 1449	1477, 1449
δ(OH), $\delta_s(CH_3)$	1340	1420 br	1423 sh, 1400 br	1419, 1383 sh	1434, 1385 sh	1419 br, 1385 sh
overtones or combinations	2920		2917	2908	2905	2903 sh

[a] See ref 37. [b] See ref 18.

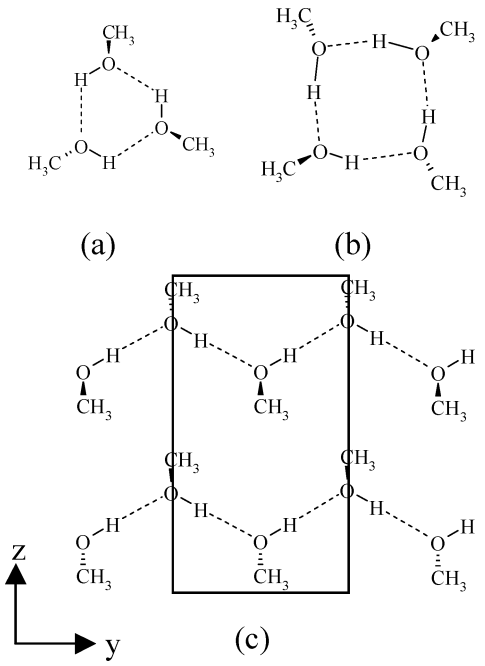

Figure 5. (a) Hydrogen bonded form of methanol: cyclic trimer and tetramer and (b) crystal structure of the α-phase of methanol; projection on the *yz* plane. The dashed lines represent hydrogen bonds.

The calculated $\delta(OH)_{op}$ bending mode of isolated OH groups in a single methanol molecule and in dimeric clusters appear at 341 and 330 cm^{-1}, respectively. Both are absent in solid methanol, as all hydroxyl groups are assumed to be hydrogen bonded. In the liquid and solid state, the molecules preferentially form chains but also form ring-like structures and zigzag chains, in which methanol is two-fold hydrogen-bonded (Figure 5). The $\delta(OH)_{op}$ torsion modes at 697 and 776 cm^{-1} show that methanol was crystallized in the low temperature α-phase.[19,35,36] This is supported by the pronounced splitting of the $\delta(OH)_{op}$ bands as compared to the single band at 655 cm^{-1} observed for liquid methanol by IR spectroscopy.[18] The doublet is due to torsional modes of hydrogen bonded methanol−hydroxyl groups of the different symmetric methanol species present in the unit cell. The band at 776 cm^{-1} is located at a lower frequency as compared to the position reported by Jobic et al.,[17] which is explained with a lower temperature ($T = 5$ K) used by these authors.

Adsorption of Methanol on Sodium Exchanged Zeolite X. In analogy to solid methanol, all hydroxyl groups of methanol adsorbed on NaX appear to be hydrogen bonded as indicated by the absence of the $\delta(OH)_{op}$ mode of freely vibrating OH groups at 330 cm^{-1}. In addition, the $\delta(OH)_{ip}$ deformation bending vibration bands of the methanol hydroxyl groups are strongly broadened and overlapped with the $\delta(CH_3)$ bending modes of the methanol methyl groups. The $\delta(OH)_{ip}$ vibrations are found at higher wavenumbers as compared to isolated methanol molecules (i.e., gas phase at 1380 cm^{-1}) by infrared spectroscopy,[18] which also supports the assumption of hydrogen bonding of the methanol hydroxyl groups. In the region of 600−900 cm^{-1}, only a broad feature of low intensity was present indicating that self-association of methanol molecules to form the crystalline α-phase did not take place. This suggests that the adsorption structure of methanol in the faujasite supercage of NaX is less ordered as compared to the solid phase. It is also possible that more than one methanol adsorption structure is formed at this loading.

The lower frequency of the broad $\delta(OH)_{op}$ bending mode (with maxima at 650 and 760 cm^{-1}) and the strong band broadening, as compared to solid methanol, suggest a less strongly hydrogen bonded structure. The broadening is attributed to the presence of a large number of perturbed methanol−hydroxyl groups differing in hydrogen bonding strength. This is also indicated by the unresolved group of bands below 450 cm^{-1} with a maximum at 95 cm^{-1} (assigned to methyl torsional and external modes). The formation of the preferred linear structure of the hydrogen bonds in methanol, realized in the methanol crystals, is sterically not possible for methanol adsorbed in the supercages of zeolite X, explaining the decreased hydrogen bonding strength.

From IR and thermogravimetric studies,[5] it has been reported that the interaction energetically controlling the sorption of methanol on alkali metal cation exchanged X zeolites is primarily the coordination of the methanol−oxygen atom to the alkali metal cation. The observation of two ν(OH) stretching modes at 3460 (shoulder) and 3341 cm^{-1} by infrared spectroscopy (Figure 4) together with the low methanol coverage (less than one molecule per cation) points to the presence of two methanol sorption structures of methanol adsorbed on NaX. These two structures of hydrogen bonded methanol molecules coordinatively bound via the methanol oxygen atom to sodium cations without methanol clustering at the exchanged cation[5] proposed are shown in Figure 6a,b.

The methanol−hydroxyl bonds of methanol adsorbed on NaX are weakened as indicated by the strong shift of the hydroxyl stretching vibrations when compared to the sharp band at 3612 cm^{-1} of relatively unperturbed methanol hydroxyl groups observed for methanol adsorbed on NaZSM-5[5] and the band at 3682 cm^{-1} for methanol in the gas phase.[37] The shoulder at 3460 cm^{-1} may result from the coordination and an additional H-bonding interaction formed between the methanol−hydroxyl group and the negatively charged zeolite oxygen atom (Figure 6a), while additional methanol−methanol interactions between methanol molecules adsorbed at neighboring cations (Figure 6b) are concluded to be most important for the appearance of the adsorption band at 3341 cm^{-1}. Note that ν(OH) stretching bands at 3293 and 3340 cm^{-1} are found for methanol tetramer clusters[38] and for liquid methanol,[39] respectively. Because of the low intensities of the $\delta(OH)_{op}$ bending modes in the INS spectrum, the presence of those two structures cannot be confirmed, but the broadening in the $\delta(OH)_{op}$ band region (600−900 cm^{-1}) supports this proposal.

Diffraction studies by Olson et al.[40] reported that 60.8 countercations are located in the faujasite supercage per unit cell for a $Na_{88}X$ zeolite. (A total of 29.8 cations are located in SIII′ positions, and 31 cations are found on SII, while none are located at SII′ and SIII; see Figure 7.) We assume that methanol will preferentially adsorb on the sodium cations located in SIII′ positions, where the cation is surrounded by two aluminum sites and a small number of next nearest-neighbor oxygen sites, which are the most basic sites in the framework.[41] These cations are the most easily accessible in the framework because they are coordinatively less saturated and have the lowest binding energy to the framework oxygen atoms. Note that for cations in SIII′ positions (two Al in four ring), an approximately 40 kJ mol^{-1} lower binding energy was determined as compared to cations in SII positions.[42,43] The weak interaction of cations in SIII′ positions and framework oxygen atoms leads to a low charge delocalization between the cations and the oxygen atoms; thus, a higher positive partial charge remains on the cations. Note that stronger adsorption was also found for CO adsorption on

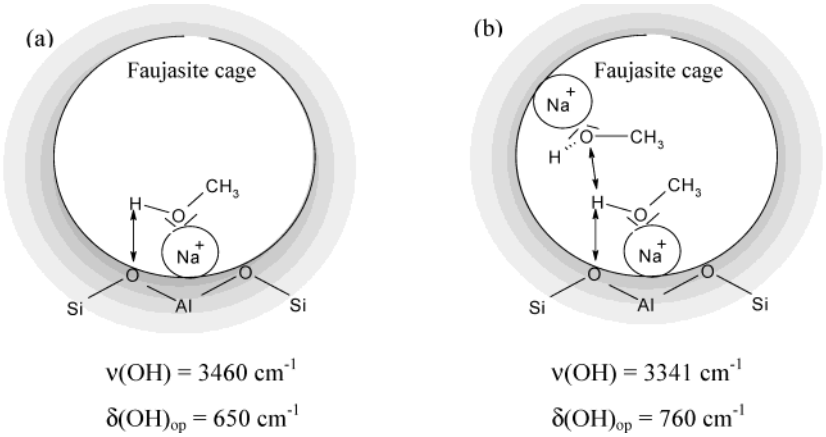

Figure 6. Schematic representation of two possible sorption structures of methanol on NaX.

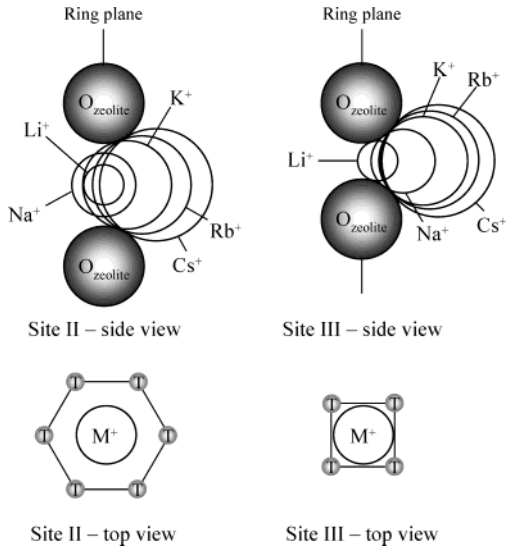

Figure 7. Shielding of alkali metal cation through oxygen atoms in the supercage on position SII and SIII;[47] T = Si, Al. (The size of the spheres represents the radii of the ions, and the distance between the oxygen atoms is based on the structure of faujasite.)

cations in SIII′ as compared to adsorption on cations in SII.[43] Because of the coverage of three molecules per supercage containing 3.7 cations on SIII′ positions, on average, we may also assume that there is no clustering at a single alkali cation.

Adsorption of Methanol on Alkali Metal Cation Exchanged Zeolite X. Changing the countercation from Na^+ to larger alkali metal cations increases the negative charge located on the framework oxygen atom of the zeolite as indicated by the Sanderson intermediate electronegativity principle (Table 1). The polarity of the zeolite framework is increased leading to enhanced base strength of the sites (lattice oxygen atoms) of Rb^+ exchanged zeolites as compared to Na^+ exchanged zeolites. The increasing framework base strength with increasing countercation size is demonstrated experimentally by infrared spectroscopy coupled with temperature programmed desorption of adsorbed probe molecules such as carbon dioxide[44,45] and pyrrole[46,47] The interactions between the slightly acidic hydroxyl of methanol and the neighboring lattice oxygen atoms increases remarkably from NaX to RbX, which leads to the formation of stronger hydrogen bonds between the methanol−hydroxyl groups and the framework oxygen atoms. As a result, the $\delta(OH)_{op}$ deformation modes are shifted to higher frequencies for a lower Lewis acid cation (for RbX at 765 and 820 cm^{-1}) as compared to NaX (650 and 760 cm^{-1}).

In addition to the increased hydrogen bond strength, with increasing size of the countercations (K, Rb, and Cs), the displacement into the faujasite cage increases[48,49] (Figure 7), leading to a decrease in the distance between coordinatively adsorbed methanol molecules in the faujasite cages. As compared to NaX, the $\delta(OH)_{op}$ bandwidths are smaller, and the frequencies of the $\delta(OH)_{op}$ vibrations are located at higher values for KX, RbX, and CsX. Those observations indicate the formation of more uniform and strongly hydrogen bonded sorption structures of methanol on zeolite samples with increasing countercation size.

In perfect agreement to the increase of the $\delta(OH)_{op}$ deformation vibration frequencies, IR spectra[5] show a shift to lower frequencies for the $\nu(OH)$ stretching modes from 3341 (Na^+) to 3220 (Rb^+) cm^{-1} (Figure 6) accompanied by an increase of the wavenumbers of the $\delta(OH)_{ip}$ deformation vibrations (not shown). This is consistent with the weakening of the methanol hydroxyl bonds with increasing framework base strength. Note that a frequency shift in the opposite direction is observed for the coordination of the methanol oxygen atom to a countercation located in an apolar zeolitic environment (e.g., on alkali metal cation exchanged ZSM-5 materials[5]) in which hydrogen bonding to the lattice does not occur. The shoulder at 3460 cm^{-1} is most dominant for NaX, while it is hardly visible for Rb and Cs exchanged X zeolites.

From both spectroscopic methods, the trends clearly indicate a strengthening of the hydrogen bonds with increasing base strength and decreasing cation Lewis acid strength, leading to a more pronounced formation of the sorption structure illustrated in Figure 5b and/or a formation of ring-like methanol structures in the supercage. DFT calculations carried out by Vayssilov et al.[50] showed that the type of cations determines the interaction between methanol and adsorption sites and that the basicity of the framework oxygen atoms near the cation influences the hydrogen bond formation and the OH stretching frequency.

A further increase in the frequency of the $\delta(OH)_{op}$ deformation vibrations and a decrease in the $\nu(OH)$ stretching frequencies for CsX as compared to RbX was not observed. The large Cs^+ cation may prevent the formation of sterically unhindered sorption complexes between methanol, cation, and pore wall in the supercage resulting in weaker hydrogen bonds, thus resulting in higher methanol hydroxyl stretching values. The peak shapes of $\nu(OH)$ and $\delta(OH)_{op}$ and their low and high frequencies nevertheless indicate the presence of intermolecular hydrogen bonds.

Alternatively, it could be speculated that the presence of sodium cations (for this material a Cs^+ exchange degree of 55.4% was reached) in the supercage lowers the average

framework polarity $-\delta_0$, (calculated in Table 1), which may decrease the hydrogen bonding strength. The exchange of zeolite NaX with cesium cations led to a preferential exchange of sodium cations at SII and SIII positions. Sodium ions are preferably located at SI and SI′ positions in the smaller cages, where Na^+ is better stabilized (due to higher coordination) at sites in the supercage.[51,52] From diffraction studies of mixed CsNaX materials with a low exchange degree, it is known that both sodium and cesium cations are located in faujasite supercages. For a $Cs_{46}Na_{50}X$ sample,[53] well-stabilized sodium cations were found to be located in SII sites, while the larger cesium cations only occupy SIII′ positions. However, recent studies of Hunger et al.[54] showed for $Cs_{46}Na_{37}X$ that a significant amount of Na^+ is located at SIII (seven ions per unit cell) and Cs^+ at SII′ (15 ions per unit cell) as well as SII (three ions per unit cell) sites. Thus, methanol may coordinate to cations on both sites in the CsX zeolite studied. Note that alkali metal exchange is not complete for the KX and RbX samples, which has also led to mixed zeolite materials. The high concentration of K^+ and Rb^+ in the exchanged X zeolites, however, ensures that the exchanged cations are present in the faujasite cages only, while the remaining sodium ions occupy only the preferred sites in the smaller cages.

The broad shoulder at high frequencies of the band below 450 cm^{-1} (Figure 3) is attributed to enhanced hydrogen bonding of the methyl hydrogen atoms to the negatively charged framework oxygen atoms, resulting in a hindered translational motion. The changes of the band shapes in the rocking vibrational modes of the methanol methyl groups also indicate a change in the steric hindrance of the methyl groups with increasing cation size probably resulting from hydrogen bond formation to the zeolite framework. Hydrogen bonding between the methanol methyl groups and the zeolite oxygen atoms is also supported by the observed red shift and increased bandwidth of the $\nu(CH_3)$ stretching vibration modes from 2957 and 2841 cm^{-1} (Na^+) to 2934 and 2820 cm^{-1} (Rb^+)[5] in the infrared spectra.

Conclusions

The combination of INS and IR spectroscopy was used to study the sorption structure of methanol on alkali metal cation exchanged faujasite (zeolite X) samples. A significant influence of the different countercations on the structural vibrations of the faujasite framework was not found. Upon cooling below 20 K, methanol crystallizes in the low temperature α-phase. In the crystalline as well as in the adsorbed phase, all methanol−OH groups appeared to be hydrogen bonded, while in the later state no self-association of methanol molecules forming the crystalline α-phase was observed. At low sorbate loading, methanol adsorbed on countercations located in SIII′ positions, the energetically preferred sites located in the supercage of zeolite X. Because of the low loading in the zeolite (three methanol molecules per 7.6 cation in the supercage, in average), clustering of more than one molecule per sorption site is not expected. The combination of INS and IR spectroscopy confirmed the presence of at least two sorption structures for methanol in alkali metal cation exchanged faujasite. Hydrogen bonding interactions between the slightly acidic hydroxyl groups of methanol and the neighboring lattice oxygen atom as well as intermolecular interactions between methanol molecules were observed. With increasing cation size, leading to increasing framework basicity, interactions between the hydrogen atoms of the hydroxyl group of methanol and the neighboring lattice oxygen atoms increased remarkably from NaX to RbX. The more uniform and strongly hydrogen bonded sorption structure points to the formation of ring-like methanol structures on these samples.

Acknowledgment. The authors thank the Deutsche Forschungsgemeinschaft (DFG) within the Sonderforschungsbereich SFB 338: Adsorption an Festkörperoberflächen: Mikroskopische Analyse von Zuständen und Prozessen Teilprojekt B9. In particular, we thank the ISIS, Rutherford Appleton Laboratory, U.K., for kindly granting measuring time to record the INS spectra.

References and Notes

(1) Lercher, J. A.; Jentys, A. *Handbook of Microporous Solids*; Schüth, F., Sing, K., Weitkamp, J., Eds.; Wiley-VCH: Weinheim, 2002; pp 1097−1156.
(2) Barthomeuf, D. *Catal. Rev. Sci. Eng.* **1996**, *38*, 521−612.
(3) Csicsery, S. M. *Zeolites* **1984**, *4*, 202−213.
(4) Palomares, A. E.; Eder-Mirth, G.; Lercher, J. A. *J. Catal.* **1997**, *168*, 442−449. Vinek, H.; Derewinski, M.; Mirth, G.; Lercher, J. A. *Appl. Catal.* **1991**, *68*, 277−284.
(5) Rep, M.; Palomares, A. E.; Eder-Mirth, G.; van Ommen, J. G.; Rösch, N.; Lercher, J. A. *J. Phys. Chem. B* **2000**, *104*, 8624−8630.
(6) www.isis.rl.ac.uk.
(7) Frisch, M. J.; Trucks, G. W.; Schlegel, H. B.; Scuseria, G. E.; Robb, M. A.; Cheeseman, J. R.; Zakrzewski, V. G.; Montgomery, J. A., Jr.; Stratmann, R. E.; Burant, J. C.; Dapprich, S.; Millam, J. M.; Daniels, A. D.; Kudin, K. N.; Strain, M. C.; Farkas, O.; Tomasi, J.; Barone, V.; Cossi, M.; Cammi, R.; Mennucci, B.; Pomelli, C.; Adamo, C.; Clifford, S.; Ochterski, J.; Petersson, G. A.; Ayala, P. Y.; Cui, Q.; Morokuma, K.; Malick, D. K.; Rabuck, A. D.; Raghavachari, K.; Foresman, J. B.; Cioslowski, J.; Ortiz, J. V.; Baboul, A. G.; Stefanov, B. B.; Liu, G.; Liashenko, A.; Piskorz, P.; Komaromi, I.; Gomperts, R.; Martin, R. L.; Fox, D. J.; Keith, T.; Al-Laham, M. A.; Peng, C. Y.; Nanayakkara, A.; Challacombe, M.; Gill, P. M. W.; Johnson, B.; Chen, W.; Wong, M. W.; Andres, J. L.; Gonzalez, C.; Head-Gordon, M.; Replogle, E. S.; Pople, J. A. *Gaussian*, Inc.: Pittsburgh, PA, 1998.
(8) Champion, D. J.; Tomkinson, J.; Kearley, G. J. *Appl. Phys. A* **2002**, *74*, S1302−S1304.
(9) Fitch, A. N.; Jobic, H.; Renouprez, A. *J. Phys. Chem.* **1986**, *90*, 1311−1318. Jobic, H.; Renouprez, A.; Fitch, A. N.; Lauter, H. J. *J. Chem. Soc., Faraday Trans 1* **1987**, *83*, 3199−3209.
(10) Sanderson, R. T. *J. Am. Chem. Soc.* **1983**, *105*, 2259−2261.
(11) Mortier, W. J. *J. Catal.* **1978**, *55*, 138−145.
(12) Jobic, H. *J. Catal.* **1991**, *131*, 293−298.
(13) Miecznikowski, A.; Hanuza, J. *Zeolites* **1985**, *5*, 188−193.
(14) No, K. T.; Bae, D. H.; Jhon, M. S. *J. Phys. Chem.* **1987**, *90*, 1772−1780.
(15) Jobic, H.; Smirnov, K. S.; Bougeard, D. *Chem. Phys. Lett.* **2001**, *344*, 147−153.
(16) Kustov, L. M.; Borovkov, V. Y.; Kazansky, V. B. *J. Catal.* **1981**, *72*, 149−159.
(17) Jobic, H. *Spectrochim. Acta* **1992**, *48A*, 293−312.
(18) Falk, M.; Whalley, E. *J. Chem. Phys.* **1961**, *34*, 1554−1568.
(19) Torrie, H. B.; Weng, S. X. *Mol. Phys.* **1989**, *67*, 575−581.
(20) Buck, U.; Siebers, J. G.; Wheatley, R. J. *J. Chem. Phys.* **1998**, *108*, 20−32.
(21) Mo, O.; Yanez, N.; Elguero, J. *J. Chem. Phys*. **1997**, *107*, 3592−3606.
(22) Hagemeister, F. C.; Gruenloh, C. J.; Zwier, T. S. *J. Phys. Chem. A* **1998**, *102*, 82−94.
(23) Huisken, F.; Kaloudis, M.; Koch, M.; Werhahn, O. *J. Chem. Phys*. **1996**, *105*, 8965−8968.
(24) Buck, U.; Ettischer, I. *J. Chem. Phys.* **1998**, *108*, 33−38.
(25) Provencal, R. A.; Paul, J. B.; Roth, K.; Chapo, C.; Casaes, R. N.; Saykally, R. J.; Tschumper, G. S.; Schaefer, H. F. *J. Chem. Phys*. **1999**, *110*, 4258−4267.
(26) Sauer, J. *J. Mol. Catal*. **1989**, *54*, 312−323.
(27) Jacobs, W. P. J. H.; van Wolput, J. H. M. C.; van Santen, R. A.; Jobic, H. *Zeolites* **1992**, *12*, 315−319.
(28) Brémard, C.; Le Maire, M. *J. Phys. Chem*. **1993**, *97*, 9695−9702.
(29) Butler, W. M.; Angell, C. L.; Allister, W. M.; Risen, W. M. *J. Phys. Chem*. **1977**, *81*, 2061−2068.
(30) Line, C. M. B.; Kearley, G. *J. Chem. Phys*. **1998**, *234*, 207−222.
(31) Jacobs, W. P. J. H.; van Wolput, J. H. M. C.; van Santen, R. A.; Jobic, H. *Zeolites* **1994**, *14*, 117−125 and references therein.
(32) Durig, J. R.; Pate, C. B.; Li, Y. S.; Antion, D. J. *J. Chem. Phys*. **1971**, *54*, 4863−4870.

(33) Aldred, B. K.; Eden, R. C.; White; J. W. *Discuss. Faraday Soc*. **1967**, *43*, 169−191.
(34) Anderson, A.; Andrews, B.; Meiering, E. M.; Torrie, B. H. *J. Raman Spectrosc*. **1988**, *19*, 85−89 and references therein.
(35) Parkes, G. S. *J. Am. Chem. Soc.* **1925**, *47*, 338−345.
(36) Weng, S. X.; Anderson, A. *Phys. Stat. Sol.* **1992**, *172*, 545−555.
(37) Serallach, A.; Meyer, R. H.; Günthard, H. *J. Mol. Spectrosc*. **1974**, *52*, 94−129.
(38) Häber, T.; Schmitt, U.; Suhm, M. A. *Phys. Chem. Chem. Phys*. **1999**, *1*, 5573−5582.
(39) Buck, U.; Huisken, F. *Chem. Rev*. **2000**, *100*, 3863−3890.
(40) Olson, D. H. *Zeolites* **1995**, *15*, 439−443.
(41) Heidler, R.; Janssens, G. O. A.; Mortier, W. J.; Schoonheidt, R. A. *J. Phys. Chem*. **1996**, *100*, 19728−19734.
(42) Buttefey, S.; Boutin, A.; Mellot-Draznieks, C.; Fuchs, A. H. *J. Phys. Chem. B* **2001**, *105*, 9569−9575.
(43) Vayssilov, G. N.; Staufer, M.; Belling, T.; Neyman, K. M.; Knözinger, H.; Rösch, N. *J. Phys. Chem. B* **1999**, *103*, 7920−7928.
(44) Jacobs, P. A.; van Cauwelaert, F. H.; Vansant, E. F.; Uytterhoeven, J. B. *J. Chem. Soc., Faraday Trans. 1* **1973**, *69*, 1056−1068.
(45) Yagi, F.; Tsuji, H.; Hattori, H. *Micropor. Mater*. **1997**, *9*, 237−245.
(46) Lavalley, J. C. *Catal. Today* **1996**, *27*, 377−401.
(47) Murphy, D.; Massiani, P.; Franck, R.; Barthomeuf, D. *J. Phys. Chem*. **1996**, *100*, 6731−6738.
(48) Huber, S.; Knözinger, H. *Appl. Catal. A* **1999**, *189*, 239−244.
(49) Cooney, R. P.; Tsai, P. *J. Raman Spectrosc*. **1979**, *8*, 195−198.
(50) Vayssilov, G. N.; Lercher, J. A.; Rösch, N. *J. Phys. Chem. B* **2000**, *104*, 8614.
(51) Mortier, W. J.; Van den Bossche, E.; Uytterhoeven, J. B. *Zeolites* **1995**, *4*, 41.
(52) Olson, D. H. *Zeolites* **1995**, *15*, 439.
(53) Shepelev, Z. F.; Butikova, I. K.; Smolin Y. I. *Zeolites* **1991**, *11*, 287−292.
(54) Hunger, M.; Schenk, U.; Buchholz, A. *J. Phys. Chem. B* **2000**, *104*, 12230.